ChemComm

COMMUNICATION

View Article Online
View Journal | View Issue

Cite this: *Chem. Commun.*, 2014, 50, 14209

Received 27th July 2014,
Accepted 19th September 2014

DOI: 10.1039/c4cc05535g

www.rsc.org/chemcomm

A lithium anode protection guided highly-stable lithium–sulfur battery†

Guoqiang Ma, Zhaoyin Wen,* Meifen Wu, Chen Shen, Qingsong Wang, Jun Jin and Xiangwei Wu

A Li_3N protection layer is fabricated on the surface of a Li anode by an *in situ* method to suppress the shuttle effect on the basis of anode protection. The discharge capacity is retained at 773 mA h g^{-1} after 500 cycles with an average coulombic efficiency of 92.3% in the electrolyte without $LiNO_3$, while the sulfur loading of the simple sulfur cathode was 2.5–3 mg cm^{-2}.

With rapid development in the field of advanced portable devices, zero-emission electric vehicles (EV) and smart grids, rechargeable batteries with high energy density and long cycle life have been in great demand.[1,2] Sulfur cathodes have high theoretical capacity (1675 mA h g^{-1}), which is ~5 times that of existing materials based on layered lithium transition metal oxides and lithium metal phosphates. In combination with natural abundance, low cost and environmental friendliness of sulfur make Li–S batteries promising candidates as the next generation power sources.[3–5]

However, the commercialization of Li–S batteries is inhibited due to the insulating nature of sulfur, volume expansion, and high solubility of lithium polysulfides (PS) in the ether-based electrolytes.[6–8] The shuttle effect originates from the diffusion of high order polysulfides to the anode side, where they react with metal lithium and form insoluble Li_2S/Li_2S_2, which irreversibly deposit on the surface of the lithium anode. Such a corrosion reaction causes the loss of active sulfur materials, leading to low coulombic efficiency, rapid capacity fading and high polarization.[9,10] Furthermore, complete conversion of sulfur to Li_2S is difficult owing to the insulating feature of Li_2S/Li_2S_2. Besides, there is some irreversible capacity for Li–S batteries because of the side reaction during the charge–discharge process.[11]

Many approaches have been made to solve the problems and improve the electrochemical performance of Li–S batteries, including the microstructural design of the cathode,[12,13] modification of the electrolyte,[10] and so on. Encapsulating sulfur into a conductive matrix[14,15] and the surface coating of sulfur or sulfur composites with conductive materials[13] are most frequently employed to address these obstacles. Conductive materials such as various forms of carbon and conductive polymers can improve the electrical conductivity of the cathode and suppress the loss of soluble polysulfide intermediates, and thereby improve the active material utilization and cycle stability.[6] In addition, the issue of low coulombic efficiency has been resolved by the addition of lithium nitrate in the electrolyte.[16] However, to date, few research studies on lithium anodes for Li–S batteries have been reported, the modification of the lithium electrode should be a new strategy to improve the performance of Li–S batteries.[6,7]

The use of Li anodes for Li–S batteries suffers from several problems. Firstly, lithium is so reactive that the electrolyte can be reduced on the surface of the Li anode to form a solid electrolyte interphase (SEI) layer easily, causing a great irreversible capacity loss and low deposition efficiency of Li upon charging.[17–19] Secondly, the Li dendrites originating from the non-uniform deposition of Li deteriorate the battery life Li-metal based batteries and even cause safety issues.[20,21] While the lithium polysulfides in the electrolyte may react with Li dendrites, thus the problem is not as serious as in the case of other Li anode based batteries.[22] Thirdly, as shown in Fig. 1a, due to the shuttle effect in Li–S batteries, the penetrating soluble lithium polysulfides through the separator react with the Li anode to form the Li_2S/Li_2S_2 layer on the surface of the lithium anode.[8,23] Then the insulating Li_2S/Li_2S_2 layer on the surface of the Li anode is difficult to be transformed into lithium polysulfides and utilized in the subsequent cycles, leading to the loss of the active material.[24] Furthermore, the insulating layer will retard the rapid diffusion of Li, resulting in poor rate capability and cycle performance.[21] Li–B alloys, lithium ion conductive solid polymer electrolytes and sulfur powder coatings have been employed to protect the Li anode during the charge–discharge process.[25–27]

Polycrystalline Li_3N has an exceptionally high Li-ion conductivity (approximately 10^{-3} S cm^{-1}) with potential application as a solid

CAS Key Laboratory of Materials for Energy Conversion, Shanghai Institute of Ceramics, Chinese Academy of Sciences, Shanghai, 200050, China.
E-mail: zywen@mail.sic.ac.cn; Fax: +86-21-52413903; Tel: +86-21-52411704

† Electronic supplementary information (ESI) available. See DOI: 10.1039/c4cc05535g

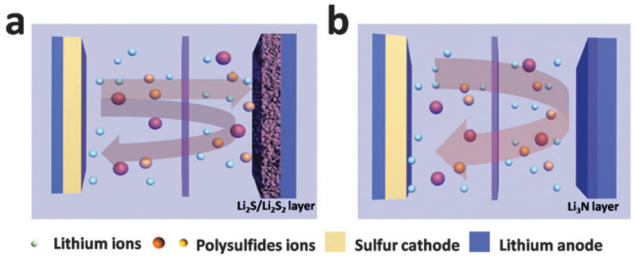

Fig. 1 Schematic of the design of a lithium metal electrode in lithium–sulfur battery configurations. (a) A battery without the Li_3N layer. (b) A battery with the Li_3N layer.

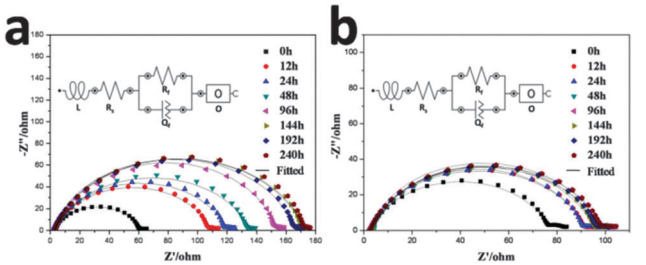

Fig. 2 AC impedance spectra of the Li/electrolyte/Li batteries with (a) as-received Li and (b) surface protected Li electrodes as a function of storage time at 25 °C.

electrolyte in lithium ion batteries.[28–30] As the closest layer to the Li metal, Li_3N can prevent the side reaction between the lithium and the carbonate-based electrolyte, promoting a stable SEI.[29] Furthermore, fast Li^+ diffusion from the electrolyte to the Li surface occurs owing to fewer reduction species in the electrolyte with Li_3N modification on the Li anode surface. Thus, it is proposed to employ Li_3N as the protective layer to address the obstacles of the Li anode for the Li–S battery discussed in this work.

Herein, as seen in Fig. 1b, a Li_3N protective layer is *in situ* fabricated on the surface of a lithium anode by the direct reaction between the Li and N_2 gas at room temperature. Firstly, a Li_3N layer has a high ionic conductivity, which does not hinder the migration of Li^+. Secondly, a Li_3N layer can prevent the side reaction between the lithium anode and the electrolyte, forming a stable SEI layer. Thirdly, the contact between the lithium polysulfides and the lithium anode is thus prevented, and the undesired corrosive reaction is suppressed. As a result, the migration of lithium polysulfides back to the cathode and their reutilization in the subsequent cycles are possible, and inhibition of capacity fading is thus realized. Furthermore, the Li dendrites originating from a non-uniform deposition of Li can be suppressed by the Li_3N layer, improving the safety of the battery.

As shown in Fig. S1 (ESI†), the phase of the Li_3N film formed on the Li surface is characterized by XRD analysis. The pure Li_3N is fabricated on the surface of Li foil by a simple method, and it is stable in the ether-based electrolyte after 10 days.[30,31] The morphologies of the as-received Li and Li_3N modified Li electrodes are given in Fig. S2 (ESI†). As seen, both electrode surfaces are homogeneous. It is noticeable that the modified surface is strongly charged by the electron beam since the Li_3N film is electronically insulated.

A lithium sheet with a Li_3N layer is beneficial in forming a stable and less resistive SEI in the carbonate-based electrolyte.[29] To investigate the interfacial stability of the Li_3N protected lithium anode in the ether-based electrolyte, AC impedance measurement for Li/electrolyte/Li batteries was performed.[17] As seen in Fig. 2, the spectra are composed of partially overlapping semicircles, corresponding to the SEI film. The equivalent circuit and related analogs fitted to the experimental data are also given in Fig. 2.

In this circuit, R_s is the electrolyte resistance, which corresponds to the high frequency intercept at the real axis. R_f is the resistance of the SEI film.[17] In the battery assembled with the primitive Li electrode, the initial resistance of the battery is less than that of the Li electrode with a Li_3N layer, indicating the existence of a protective layer on the surface of the lithium anode. However, the R_f value increases from 59 Ω to 168 Ω after 144 h, owing to the gradual growth of SEI between the lithium electrode and the electrolyte. In the battery assembled with the Li_3N protected Li electrode, R_f initially increases to the maximum value after 48 h and stabilizes at around 92 Ω R_f stabilizes at a lesser value after a shorter storage time compared to that of the as-received Li anode, indicating the suppressed undesired side reactions between the Li_3N protected lithium electrode and the ether-based electrolyte. As a result, the interfacial stability of the lithium electrode is improved by the formation of a Li_3N protection layer.

The fitted results of the impedance spectra shown in Fig. 2a and b are given in Tables S1 and S2 (ESI†), respectively. Among them, $B = l/D^{1/2}$, where l is the length of the stagnant layer and D is the diffusion coefficient. According to the previous studies, the diffusion coefficient of Li^+ in the electrolyte is about 3.4×10^{-6} cm^2 s^{-1}, thus the value of l can be calculated.[32] As shown, the goodness fit for the whole electrode system is represented by the chi-square (χ^2) parameter. By comparing R_f and Q_f in the two tables, it can be seen that the SEI formed on the Li_3N protected Li anode surface is smoother and less resistive. As the Li_3N protective layer is formed previously and is used as the closest layer to the Li sheet, it can effectively prevent the side reactions between Li and the electrolyte. Moreover, the high Li conductivity of Li_3N can provide much smaller Li^+ migration resistance R_f. The larger value Y_0 of "Cothyperbol" element O and shorter lengths of stagnant layers suggest fast Li^+ diffusion from the electrolyte to the Li surface, owing to fewer reduction species in the electrolyte with Li_3N modification.

The cyclic voltammogram (CV) profiles were measured to identify the redox reactions for the battery with different anodes (Fig. S3a and b, ESI†). The electrochemical activation of the Li_3N protected anode was not as obvious as that of the primitive Li anode. This can be ascribed to the faster Li^+ diffusion from the electrolyte to the Li surface with the modification of Li_3N, owing to fewer reduction species in the electrolyte with Li_3N modification, which is consistent with the results of AC impedance.

In a coin-type battery for the electrochemical test, the lithium anode is normally far from sufficient with respect to the active material in the sulfur cathode, so the initial discharge capacity is determined by the state of the sulfur cathode. As seen in Fig. 3a,

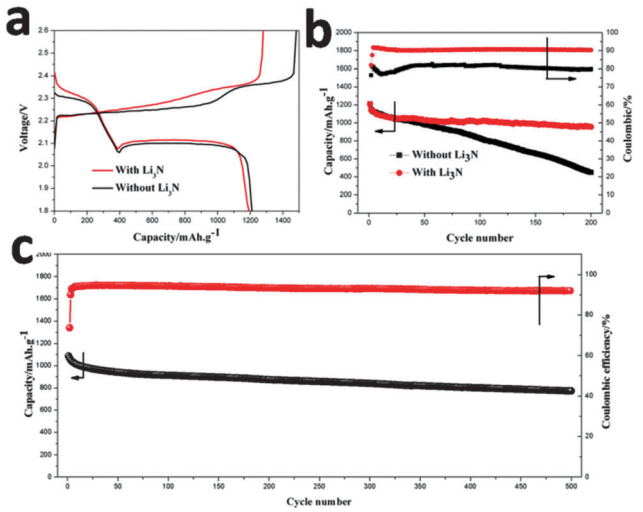

Fig. 3 The initial charge–discharge profiles of Li–S batteries with different lithium anodes at 0.2 C (a), the cycle performance and coulombic efficiencies of Li–S batteries at 0.2 C with different lithium anodes (b), the prolonged cycle performance and coulombic efficiencies of Li–S batteries at 0.5 C with the Li_3N layer protected Li anode (c).

the Li–S battery with a primitive Li electrode shows an initial discharge capacity comparable with that of the Li–S battery with a Li_3N protected lithium anode. However, the two discharge potential plateaus of the battery with a Li_3N protected anode are higher than those of the battery with a primitive Li anode, meanwhile the charge potential plateau is lower for the battery with a Li_3N protected anode, further proving lower polarization of the Li_3N protected anode in the ether-based electrolyte.

The cycle performance and coulombic efficiencies of Li–S batteries at 0.2 C with different lithium electrodes are shown in Fig. 3b. As mentioned above, once a lithium anode is protected by a Li_3N layer, the contact between the lithium anode and lithium polysulfides can be restricted, so the corrosive reaction between them during the discharge process is suppressed effectively. Furthermore, because of the high Li^+ conductivity of Li_3N, more insulating Li_2S/Li_2S_2 aggregated on the surface of the conductive Li_3N layer will transform to the soluble Li_2S_x during the charge process. Consequently, the so called "shuttle effect" is largely restricted, thus the low coulombic efficiencies, redistribution of active materials and rapid capacity fading are suppressed significantly. As shown, the discharge capacity of the Li–S battery with a Li_3N protected Li anode remains as high as 956.6 mA h g^{-1} at 0.2 C with a capacity retention of 79.7% after 200 cycles, while the Li–S battery with a primitive Li anode shows a capacity of 452.2 mA h g^{-1} at 0.2 C with a capacity retention of only 37.2%. It is noticeable that the average coulombic efficiency of the Li–S battery with a protected Li anode is as high as 91.4% in the electrolyte without $LiNO_3$, which is much higher than 80.7% for the Li–S battery with a primitive Li anode. Moreover, the Li–S battery with the protected Li anode also shows excellent prolonged cycle performance at 0.5 C. Over 500 cycles, the capacity retention of 71.1% (from 1087.2 to 773 mA h g^{-1}) is obtained, the decay rate is as low as 0.0578% per cycle, and the average coulombic efficiency is 92.3%. The charge–discharge profiles of the battery with a protected Li anode are displayed in Fig. S4 (ESI†). There is no evident evolution of the curves during the prolonged cycles, indicating the high reversibility of the electrochemical reaction during the charge–discharge process. Although the addition of $LiNO_3$ in the electrolyte can increase the coulombic efficiency of a Li–S battery, it was reported that $LiNO_3$ was reduced on the cathode below 1.5 V, and that the formed products severely affected the reversibility of the sulfur cathode. Moreover, it is gradually consumed on the Li anode, which leads to a decrease in the protection efficiency, and it is a strong oxidative agent, which could cause a safety issue when a high concentration is used, especially at high temperature.[10] The Li–S battery with the Li_3N modified Li anode shows excellent cycle stability and improved coulombic efficiency in the electrolyte without $LiNO_3$, thus avoiding the disadvantages of $LiNO_3$ additives.

Because lithium polysulfides are dissolved in the ether-based electrolyte once formed, they migrate in the electrolyte and reach the surface of the lithium anode, followed by an immediate reaction with the metallic-lithium anode and the formation of Li_2S/Li_2S_2.[21] This results in the rapid loss of the active material and serious anode corrosion. Therefore, the self-discharge of Li–S batteries is much more serious than that of the conventional Li-ion batteries. However, as seen in Fig. S5 (ESI†), the self-discharge behavior is effectively suppressed by protection of the Li anode with Li_3N.

As shown in Fig. S6 (ESI†), a Li_3N layer on the surface of a lithium anode restricts the contact of the lithium anode and lithium polysulfides, the suppressed corrosive reaction promotes more lithium polysulfides to be reutilized in the subsequent cycles, thus the redistribution of the insulating active material is suppressed effectively. Therefore, the decreased resistance is obtained for the Li–S battery with a Li_3N protected Li anode after 100 cycles.

Fig. S7 (ESI†) compares the surface morphologies of the Li anode with and without a Li_3N protection layer after 100 cycles. The corrosive reaction between lithium polysulfides and the Li anode results in severe damage during the charge–discharge process for a primitive Li anode, which increases the resistance of the battery and accelerates the capacity fading. As seen in Fig. 4a–c, the thickness of the Li_2S_2/Li_2S layer on the surface of a primitive lithium anode is as high as 100 μm, and the interface between the Li and Li_2S_2/Li_2S layer is uneven.[24] However, as seen in Fig. 4d–f, the thickness of the Li_2S_2/Li_2S layer is only about 10 μm in the protected Li anode, only about 1/10 that of the primitive lithium anode. In addition, the contact area between the Li_3N protected Li anode and the Li_2S/Li_2S_2 layer is relatively small, indicating that the undesired corrosive reaction is suppressed effectively when the lithium anode is protected by a Li_3N layer.

In summary, a Li_3N protection layer is successfully fabricated on the surface of a Li anode through a simple and novel method at room temperature. The protected Li anode shows high stability in the electrolyte compared with the primitive Li anode. As an anode of a Li–S battery, the protected Li shows an enhanced cycle performance. Firstly, the protective layer has high Li^+ conductivity, which does not affect the diffusion kinetics of Li^+. Secondly, the Li_3N layer

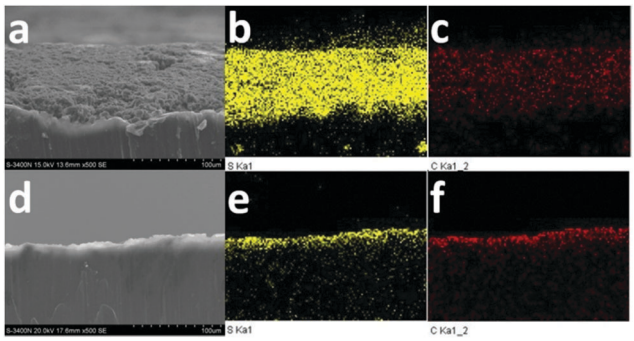

Fig. 4 The cross section morphologies (a and d) and EDS mapping element of sulfur (b and e) and carbon (c and f) of a primitive Li anode and the Li_3N protected Li anode after 100 cycles.

on the surface of the Li anode is beneficial to suppress the undesired side reactions between the Li anode and the electrolyte, forming a smooth and less resistive SEI. Thirdly, the Li_3N layer can separate the contact between Li metal and lithium polysulfides, thus the corrosive reaction between them is inhibited effectively. Finally, the protective layer on the surface of a Li anode can suppress the growth of Li dendrites originating from a non-uniform deposition of Li, improving the safety of Li–S batteries.

This work was financially supported by the NSFC Project No. 51373195, 51201177 and 51272267; research projects from the Science and Technology Commission of Shanghai Municipality No. 08DZ2210900.

Notes and references

1 S. A. F. Peter, G. Bruce, L. J. Hardwick and J.-M. Tarascon, *Nat. Mater.*, 2012, **11**(1), 19.
2 H. B. Dunn, H. Kamath and J. M. Tarascon, *Science*, 2011, **334**(6058), 928.
3 X. Ji and L. F. Nazar, *J. Mater. Chem.*, 2010, **20**, 9821.
4 J. W. Kim, J. D. Ocon, D. W. Park and J. Lee, *ChemSusChem*, 2014, 7(5), 1265.
5 H. Kim, H.-D. Lim, J. Kim and K. Kang, *J. Mater. Chem. A*, 2014, **2**, 33.
6 Y. Yang, G. Zheng and Y. Cui, *Chem. Soc. Rev.*, 2013, **42**, 3018.
7 Y. X. Yin, S. Xin, Y. G. Guo and L. J. Wan, *Angew. Chem., Int. Ed.*, 2013, **52**(50), 13186.
8 Y. Fu, A. Manthiram and Y. S. Su, *Acc. Chem. Res.*, 2012, **46**(5), 1125.
9 S. Evers and L. F. Nazar, *Acc. Chem. Res.*, 2013, **46**, 1135–1143.
10 S. S. Zhang, *J. Power Sources*, 2013, **231**, 153.
11 Y. Diao, K. Xie, X. Hong and S. Xiong, *Acta Chim. Sin.*, 2013, **71**, 508.
12 X. Chen, Z. Xiao, X. Ning, Z. Liu, Z. Yang, C. Zou, S. Wang, X. Chen, Y. Chen and S. Huang, *Adv. Energy Mater.*, 2014, DOI: 10.1002/aenm.201301988.
13 G.-C. Li, G.-R. Li, S.-H. Ye and X.-P. Gao, *Adv. Energy Mater.*, 2012, **2**, 1238.
14 X. L. Ji, K. T. Lee and L. F. Nazar, *Nat. Mater.*, 2009, **8**, 500.
15 J. Zhang, H. Ye, Y. Yin and Y. Guo, *J. Energy Chem.*, 2014, **23**, 308.
16 X. Liang, Z. Y. Wen, Y. Liu, M. F. Wu, J. Jin, H. Zhang and X. W. Wu, *J. Power Sources*, 2011, **196**, 9839.
17 I. S. Kang, Y. S. Lee and D. W. Kim, *J. Electrochem. Soc.*, 2013, **161**, A53.
18 D. J. Lee, H. Lee, J. Song, M. H. Ryou, Y. M. Lee, H. T. Kim and J. K. Park, *Electrochem. Commun.*, 2014, **40**, 45.
19 J. B. Goodenough and K.-S. Park, *J. Am. Chem. Soc.*, 2013, **135**, 1167–1176.
20 R. D. Rauh, K. M. Abraham, G. F. Pearson, J. K. Surprenant and S. B. Brummer, *J. Electrochem. Soc.*, 1979, **126**, 523.
21 Y. V. Mikhaylik and J. R. Akridge, *J. Electrochem. Soc.*, 2004, **151**, A1969.
22 D. Aurbach, E. Pollak, R. Elazari, G. Salitra, C. S. Kelley and J. Affinito, *J. Electrochem. Soc.*, 2009, **156**, A694.
23 S. S. Zhang, *J. Power Sources*, 2013, **231**, 153.
24 J. Zheng, M. Gu, M. J. Wagner, K. A. Hays, X. Li, P. Zuo, C. Wang, J. G. Zhang, J. Liu and J. Xiao, *J. Electrochem. Soc.*, 2013, **160**, A1624.
25 R. Demir-Cakan, M. Morcrette, Gangulibabu, A. Guéguen, R. Dedryvère and J.-M. Tarascon, *Energy Environ. Sci.*, 2013, **6**, 176.
26 Y. M. Lee, N.-S. Choi, J. H. Park and J.-K. Park, *J. Power Sources*, 2003, **119–121**, 964.
27 B. Duan, W. Wang, H. Zhao, A. Wang, M. Wang, K. Yuan, Z. Yu and Y. Yang, *ECS Electrochem. Lett.*, 2013, **2**, A47.
28 U. v. Alpen, A. Rabenau and G. H. Talat, *Appl. Phys. Lett.*, 1977, **30**, 621.
29 M. Wu, Z. Wen, Y. Liu, X. Wang and L. Huang, *J. Power Sources*, 2011, **196**, 8091.
30 Y. Yan, J. Y. Zhang, T. Cui, Y. Li, Y. M. Ma, J. Gong, Z. G. Zong and G. T. Zou, *Eur. Phys. J. B*, 2008, **61**, 397.
31 S. Cui, W. Feng, H. Hu, Z. Feng and Y. Wang, *Solid State Commun.*, 2009, **149**, 612.
32 Y. C. Chang and J. H. Jong, *J. Chin. Inst. Chem. Eng.*, 2004, **35**, 425.

